BUTTERWORTH HEINEMANN

A quantitative analysis of heat transfer regimes in gas–solid fluidized beds

J. D. Lu* and G. Flamant
Institut de Science et de Génie des Matériaux et Procédés, Centre National de la Récherche Scientifique, Font-Romeu, France

On the basis of a new theoretical model recently proposed by the authors for heat transfer between walls and fluidized beds, a quantitative analysis on heat transfer regimes is presented in this paper. From the dimensionless, differential equations describing the heat transfer modes; i.e., conduction, convection, and radiation is mainly determined by the characteristic numbers: Archimedes number, Ar; and Planck number, N^*. It is found that the convection in laminar regime and conduction in turbulent regime are still non-negligible components. A heat transfer diagram in a Archimedes number *versus* Planck number is proposed. Nine domains are defined according to the variation of the dominant heat transfer mechanism.

Introduction

It is well known that the magnitudes of heat transfer modes; i.e., conduction, convection, and radiation between a fluidized bed and an immersed surface, vary with particle diameter and temperature. Several definitions have been proposed for the determination of heat transfer regimes in which one or two modes are dominant mechanisms.

Decker and Glicksman (1981) suggested a classification based on the comparison between the thermal time constant of the particles (t_{th}) and the mean contact time of the particles at the wall (t_c). For small particle beds, $t_c \gg t_{th}$, $d_p < 400\ \mu m$, heat transfer is dominated by conduction (also termed the particle convection, the adequacy of this definition will be discussed in this paper). For large particle beds, $t_c \ll t_{th}$, $d_p > 1500\ \mu m$, the heat transfer is, to a large extent, caused by gas convection and, as a first approximation, the particle temperature change is negligible. For intermediate particles, both conduction and convection must be considered. Jovanovic and Catipovic (1983) also proposed a similar definition of thermally small and large particles. The difference is only the particle thermal time constant that is twice of that calculated by Decker and Glicksman.

Saxena and Ganzha (1984) classified the particles into three groups. For their group I, which is defined by $Re_{mf} < 10$ and $Ar < 2.17 \times 10^4$, conduction through emulsion is the dominant mechanism of heat transfer, and the fluid flow through the emulsion is laminar. For the group III of large particles characterized by $Re_{mf} \geq 200$ and $Ar \geq 1.60 \times 10^6$, the heat transfer is strongly controlled by the convection part caused by the turbulent flow around the particles, and the conductive component is only a negligible part. The transitional group II characterized by Re_{mf} ranging from 10 to 200 and Ar ranging from 21,700 to 1.6×10^6 was divided by Saxena and Ganzha into two subgroups: IIa, $21{,}700 \leq Ar \leq 1.3 \times 10^5$ in which the convection part of h_w is not negligible compared with the conduction part and IIb, $1.3\ 10^5 \leq Ar \leq 1.6\ 10^6$ in which the two components are comparable with each other.

Because the effect of temperature on the transition between regimes and the radiation mode was not accounted for in the previous classifications, Flamant et al. (1992a) presented a new definition of the heat transfer regimes as a function of temperature and particle diameter. The analysis was based on the Saxena and Ganzha's (1984) classification combined with Ergun's equation. For the radiative transfer, the Planck number was used for small particle beds, and a convection/radiation interaction number was introduced for large particle beds where the convection term accounts for particle and gas contribution.

However, the real significance and importance of each heat transfer mechanism in transient heat exchange procedure and in different regimes cannot be found in the previous classifications because of the lack of a generalized model or correlations usable in a large range of particle diameter and operating conditions. A general equation was derived by Kunii and Levenspiel (1992) and a set of correlations was presented by Borodulya et al. (1991) that seem valid over a wide range of experimental conditions, although the later seems to be adequate for the particulate beds. At the same time, a new theoretical model was proposed recently by the authors Lu et al. (1993) and Flamant et al. (1993), which considered all heat transfer modes and seems to be suitable as an analysis tool for heat transfer mechanisms in fluidized beds. Thus, this paper attempts to make a mechanismic and quantitative analysis of the heat transfer regimes mainly based on this model.

Summary of the theoretical model

Using the heterogeneous theory and the concept of variable property boundary layer for the emulsion phase, a generalized

* Present address, Dept. of Power Engineering, Huazhong University of Science and Technology, Wuhan, Hubei, 430074 P.R. of China.

Address reprint requests to G. Flamant, Centre National de la Récherche Scientifique, Ave. du Professeur Trombe, BP.5, ODEILLO, F. 66125 Font-Romeu, Cedex, France.

Received 1 January 1994; accepted 18 November 1994

Int. J. Heat and Fluid Flow 16: 131–138, 1995

655 Avenue of the Americas, New York, NY 10010

SSDI 0142-727X/95/$10.00
SSDI 0142-727X(94)00018-8

theoretical model describing heat transfer in gas–solid bubbling fluidized beds with heat exchange walls was presented in Lu et al. (1993). Three heat transfer modes (i.e., conduction, convection, and radiation) were all accounted for, and it was proved that this model can be used for the large and small particle beds (groups B and D of Geldart's (1973) classification). Because the result was given in dimensional form, it is difficult to analyze systematically the dominant mechanisms in different situations. Thus, we rewrite here the differential equations given in Flamant et al. (1993) that describe the transient heat transfer process occurring when the wall T_w contacts with a packet of particles at the bed temperature T_B, but in dimensionless form

Momentum equation for the gas phase

$$-\frac{\mu_g}{\mu_{gB}}\frac{\delta_{eB}}{\delta}\frac{K_{eB}}{d_p^2\delta_{eB}}\frac{d^2V}{dX^2}+\frac{\mu_g}{\mu_{eB}}\frac{K_{eB}}{K}V+\frac{\rho_g}{\rho_{gB}}\frac{C}{C_{gB}}\mathrm{Re}_{Kc}V^2=1+\mathrm{Re}_{Kc} \tag{1}$$

where K and C are the permeability and inertia coefficient of the emulsion phase; Re_{KC} is the modified Reynolds number defined as $K_{eB}C_{eB}\langle v\rangle_{eB}/\nu_{gB}$.

Energy equation for the gas phase

$$\frac{\partial}{\partial \mathrm{Fo}_m}\left[(\delta-\delta_{st})\frac{(\rho C_p)_g}{(\rho C_p)_s}\theta_g\right]+\mathrm{Re}_m\mathrm{Pr}_m\frac{(\rho C_p)_g}{(\rho C_p)_{gm}}V\frac{\partial\theta_g}{\partial Y}=\frac{\partial}{\partial X}\left(\frac{\lambda_{ge}}{\lambda_{gm}}\frac{\partial\theta_g}{\partial X}\right)+\frac{6(1-\delta)}{\Phi_P}\frac{\lambda_g}{\lambda_{gm}}\mathrm{Nu}_{gP}(\theta_P-\theta_g) \tag{2}$$

Energy equation for the particle phase

$$\frac{\partial}{\partial \mathrm{Fo}_m}\left\{\left[(1-\delta)+\delta_{st}\frac{(\rho C_p)_g}{(\rho C_p)_s}\right]\theta_P\right\}=\frac{\partial}{\partial X}\left(\frac{\lambda_{Pe}}{\lambda_{gm}}\frac{\partial\theta_P}{\partial X}\right)-\frac{6(1-\delta)}{\Phi_P}\frac{\lambda_g}{\lambda_{gm}}\mathrm{Nu}_{gP}(\theta_P-\theta_g)-\frac{1}{N_m^*}\tau_B\tau\left[\left((1-\omega)\theta_P^4-\frac{\pi}{2}\int_{-1}^{1}I\,\mathrm{d}\mu\right)\right] \tag{3}$$

In the two energy equations above, the gas phase is divided into two parts—the moving part ($\delta-\delta_{st}$) and the stagnant part δ_{st}; that is, fillets surrounding the contact points between adjacent particles and are assumed to be in thermal equilibrium with particles. Nu_{gP} is the interphase heat transfer Nusselt number between gas and particles and $N_m^*=\lambda_{gm}\kappa_e/4\sigma T_m^3$ is a modified Planck number indicating the relative importance of conduction and radiation.

Because the heat transfer in fluidized beds obviously is affected by the conductivity of gas phase near the wall, this modified Planck number is defined on the basis of the mean gas conductivity and the extinction coefficient of the emulsion; whereas, the classical definition used both properties related to emulsion (for example, in Flamant et al. 1992a). λ_{ge} and λ_{pe} are the equivalent conductivities of gas phase and particle phase, respectively, and $\tau=\kappa d_p$ is the optical thickness of the one particle bed depth (κ is the extinction coefficient calculated by $\kappa=1.5(1-\delta)/d_p$ and $\kappa_e=1.5(1-\delta_{eB})/d_p$). The subscript m indicates that the thermal properties are determined with respect to the mean temperature $T_m=(T_B+T_w)/2$ as reference temperature.

Notation

Ar Archimedes number, $gd_P^3\rho_{gB}(\rho_s-\rho_{gB})/\mu_{gB}^2$
C inertia coefficient of the emulsion phase
C_P specific heat
d_P particle diameter
f_b fraction of bubble phase
Fo Fourier number, $\lambda_{gm}t/[(\rho C_P)_s d_P^2]$
K permeability of emulsion phase
L dimensionless longitudinal length of the wall contacted by the emulsion packet, l/d_P
N^* modified Planck number, $\lambda_{gm}\kappa_e/4\sigma T_m^3$
Nu Nusselt number, hd_P/λ_g
P particle scattering function
R ratio of heat transfer component
Pr Prandtl number, $C_{Pg}\mu_g/\lambda_g$
Re Reynolds number, $\langle v\rangle_{eB}d_P\rho_g/\mu_g$
T temperature
t time
V dimensionless velocity, $\langle v\rangle/\langle v\rangle_{eB}$
X dimensionless transverse coordinate, x/d_P
Y dimensionless longitudinal coordinate, y/d_P

Greek

δ porosity
ε emissivity
θ dimensionless temperature, T/T_m
κ extinction coefficient $1.5(l-\delta_e)/d_P$
λ thermal conductivity
μ dynamic viscosity or cosine of angle between directions of propagation and observation
ν kinematic viscosity
ρ density
σ Stefan–Boltzmann constant
σ_S scattering coefficient
τ optical thickness of one particle bed depth, κd_P
Φ_P particle sphericity
ω scattering albedo, σ_S/κ

Subscripts

B properties far from the wall
b bubble phase
c contact time
d conduction
e emulsion phase or effective value
g gas phase
m thermal properties with respect to the mean temperature, $T_m=(T_B+T_W)/2$
mf minimum fluidization
o output part of heat
op optimum value
p particle phase
r radiation
s solid or stored part of heat
st stagnant part of gas
th thermal constant
V convection
w wall

Superscripts

o state with $\langle V\rangle=0$

I is the dimensionless radiation intensity that is the solution of the following radiation intensity equation

$$\mu \frac{\partial I}{\tau \partial X} = -I + \frac{(1-\omega)}{\pi}\theta_P^4 + \frac{\omega}{2}\int_{-1}^{1} I(\mu')P(\mu')\,d\mu' \tag{4}$$

where P is the scattering phase function, defined by the scattering properties of individual particles.

Because the superficial velocity in the emulsion phase far the wall is assumed to be equal to U_{mf}, the Ergun equation is needed:

$$\frac{150(1-\delta_{eB})}{\phi_P^2\delta_{eB}^3}\mathrm{Re}_{mf} + \frac{1.75}{\phi_P\delta_{eB}^3}\mathrm{Re}_{mf}^2 = \mathrm{Ar} \tag{5}$$

The thermal properties in Re_{mf} and Ar in the above equations are calculated with respect to bed temperature because the hydrodynamics in bed bulk is determined by the bed temperature.

Because the governing equations given above are in integral–differential form, some special treatments must be developed to obtain the solution of the equations. The discrete-ordinate method can be taken as an exact solution when the number of ordinates increases. The two-flux method was also checked by Flamant et al. (1994) and compared with the results of discrete-ordinate method. It was found that the differences between the two methods are small in general cases; therefore, the two-flux method is used in this paper because of the shorter calculating time needed. Combined with the necessary boundary conditions and correlations for porosity distribution $\delta(X)$, equivalent conductivities of gas phase and particle phase λ_{ge}/λ_g, λ_{pe}/λ_p and gas–particle interphase heat transfer given and discussed by Lu et al. (1993), as shown in Appendix B, the numerical solution of Equations 1–5 predicts the distributions of particle and gas temperatures and the radiation fluxes. Then the heat transfer coefficients of gas phase, particle phase, and radiation, which have been averaged over the contact time and the longitudinal distance of heat transfer wall contacted by emulsion phase, can be predicted by the following definitions:

$$\mathrm{Nu}_{ei} = \frac{1}{L\mathrm{Fo}}\int_0^L\int_0^{\mathrm{Fo}} \left.\frac{\partial\theta_i}{\partial X}\right|_{X=0} d\mathrm{Fo}\cdot dY \qquad (i = g, p) \tag{6}$$

$$\mathrm{Nu}_{er} = \frac{1}{L\mathrm{Fo}}\int_0^L\int_0^{\mathrm{Fo}} \varepsilon_w\left\{\sigma\theta_w^4 - 2\pi\int_{-1}^{0} I\cdot\mu\,d\mu\right\} \Big/ (\theta_w - \theta_B)\cdot d\mathrm{Fo}\cdot dY\,\frac{d_p}{\lambda_{gm}} \tag{7}$$

Although the aim of this model is to describe the heat transfer in bubbling fluidized beds, the heat transfer Nusselt numbers predicted by Equations 6 and 7 are only valid for the period when the wall contacts emulsion packets. When the wall contacts bubbles, heat is also transferred between the wall and the fluidized bed. In general, the heat transfer caused by the gas convection when the wall contacts bubbles is much smaller than the other components, except at high pressure or in the freeboard region, therefore it is omitted in this paper as a first approximation.

The radiative heat transfer of bubble phase must be accounted for because the temperature of bubble boundary does not change when emulsion packets contact the wall, especially the equivalent emissivity of bubbles is larger than the equivalent emissivity of emulsion phase caused by the concave shape of bubbles, which results in $\mathrm{Nu}_{br} \geq \mathrm{Nu}_{er}$. For the semispherical bubble and a transparent gas, the radiative heat transfer Nusselt number of bubble phase can be calculated by the following formula:

$$\mathrm{Nu}_{br} = \frac{2\sigma(\theta_w^4 - \theta_B^4)}{\left[\left(\frac{2}{\varepsilon_w} + \frac{1}{\varepsilon_e} - 1\right)(\theta_w - \theta_B)\right]}\frac{d_P}{\lambda_{gm}} \tag{8}$$

Finally, the overall heat transfer coefficient between the wall and the fluidized bed can be calculated by the following:

$$\begin{aligned}\mathrm{Nu}_w &= (1-f_b)(\mathrm{Nu}_{ep} + \mathrm{Nu}_{eg} + \mathrm{Nu}_{er}) + f_b\mathrm{Nu}_{br} \\ &= (1-f_b)\mathrm{Nu}_e + f_b\mathrm{Nu}_b\end{aligned} \tag{9}$$

The time fraction during which the wall is in contact with the bubble phase f_b and the contact time of emulsion packets at the wall t_e are needed for the determination of the heat transfer Nusselt number Nu_w, which are dependent on the hydrodynamics of the bed. Because the aim of this paper is to discuss the heat transfer regimes, we only consider the maximum heat transfer at ambient temperature. There exist several correlations for the prediction of the optimum flow-rate. The correlations proposed by Chen and Pei (1985) are adopted here,

$$\mathrm{Re}_{\mathrm{opt}} - \mathrm{Re}_{mf} = 0.215\mathrm{Ar}^{0.44} \qquad 20 < \mathrm{Ar} < 210^4 \tag{10a}$$

$$\mathrm{Re}_{\mathrm{opt}} - \mathrm{Re}_{mf} = 0.060\mathrm{Ar}^{0.52} \qquad 2\,10^4 < \mathrm{Ar} < 10^7 \tag{10b}$$

The bubble fraction f_b is determined by Borodulya et al.'s (1985) correlation.

$$f_b = \frac{\delta - \delta_{mf}}{1-\delta_{mf}} = 1.56\frac{\mathrm{Re} - \mathrm{Re}_{mf}}{\mathrm{Ar}^{1/2}} \tag{11}$$

The contact time of emulsion phase with the wall is a parameter rather difficult to determine, and the predictions of available correlations (Baskakov et al. 1973; Thring 1977) differ seriously between each other. From the observation of experimental results (Ozkaynak and Chen 1980; Lu 1988), it can be found that the contact time t_e is generally in the range of 0.1–0.3 s for standard fluidizing conditions, so we choose $t_e = 0.2$ s for the calculation.

Discussion on heat transfer regimes

From Equations 1–5, the solution of the temperature and radiation flux distributions can be obtained, and they are functions of the following dimensionless groups:

$$\mathrm{Fo}_m,\ \mathrm{Ar},\ N_m^*,\ \mathrm{Pr}_m,\ \frac{(\rho C_P)_{gm}}{(\rho C_P)_s},\ \frac{\lambda_s}{\lambda_{gm}},\ \delta_{mf},\ \phi_P,\ \frac{T_w}{T_B},\ \varepsilon_w,\ \varepsilon_P,\ X,\ Y \tag{12}$$

The heat transfer Nusselt numbers can be predicted as functions of the same parameters.

The heat transfer regimes are discussed in this paper for beds of sand fluidized by air, because this case is frequently considered in experimental and theoretical research. The thermal properties of air and sand, as well as some other basic parameters are listed in the Appendix A. With the specific hydrodynamic situations determined by Equations 10 and 11, the heat transfer Nusselt numbers are only related to the Archimedes number and modified Planck number.

Definition of conduction and convection heat transfer modes

The heat transfer Nusselt numbers calculated by Equation 6 represent the heat exchanged through the interphase of the wall with the gas phase and the particle phase, which are termed as gas component and particle component, respectively. They are determined by the temperature distribution of each phase near

the wall. When drawing attention to the energy Equations 2 and 3, it can be seen that the temperature distributions are affected by conduction and convection, as well as radiation at high temperature, that occur simultaneously (in parallel and series). Therefore, the discussion about the heat transfer regimes in which one or two transfer modes are dominant should be based on a specific definition of conduction and convection. In this paper, we make the definitions of conduction and convection components as follows.

Conduction component Nu_{ed}. Heat transferred during the contact time of emulsion phase at the wall when the interstitial fluid velocity is set zero. At the high temperature condition, it should be the difference of $Nu_{e,dr}$ and Nu_{er}.

Convection component Nu_{ev}. The increase of heat transfer when the interstitial fluid velocity is taken into account; i.e., the difference of Nu_e and Nu_{ed} or Nu_e and $Nu_{e,dr}$ at high temperature.

Thus, the formula for calculating the total Nusselt number of Equation 9 can be rewritten as follows:

$$Nu_w = (1 - f_b)(Nu_{ed} + Nu_{ev} + Nu_{er}) + f_b Nu_{br} = Nu_d + Nu_v + Nu_r \quad (13)$$

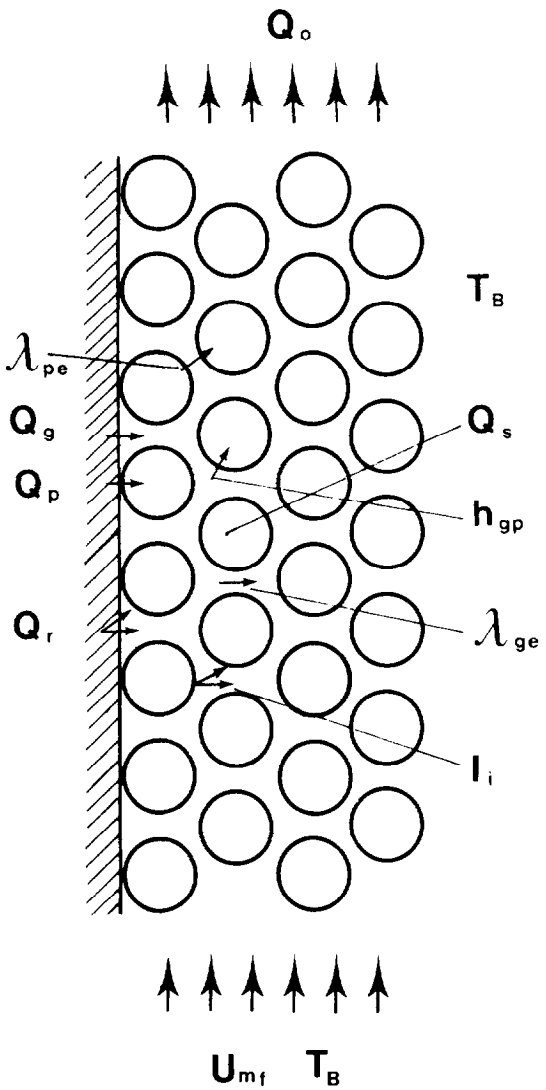

Figure 1 Heat transfer mechanisms when emulsion packet contacts wall

where $Nu_d = (1 - f_b)Nu_{ed}$ $Nu_v = (1 - f_b)Nu_{ev}$ and $Nu_r = (1 - f_b)Nu_{er} + f_b Nu_{br}$.

In many previous studies (e.g., Saxena and Ganzha 1984), the conduction component was also termed the particle convection because particles absorb or release heat when emulsion packets contact the wall and its seems mainly due to the conduction mode. Though there is no convection term in the energy Equation 3 for particle phase, it is affected by the gas convection through the interphase heat transfer between the fluidizing fluid and particles. A physical diagram of heat transfer procedure when the emulsion phase is contacting the wall can be given as shown in Figure 1. The heat is transferred through the interface between the wall and the contacting emulsion packet as the sum of particle component, gas component, and radiation component on the basis of the heat exchange mechanisms of conduction, convection, and radiation. One part of the heat is carried out by the fluidizing fluid that passes through the emulsion phase, the other part is redistributed between the two phases by diffusion (in each phase), interphase heat exchange and radiation. As a result of the processes, the temperatures of gas and particles in the emulsion packet change. The thermal energy increment (or decrement) of the emulsion packet during its contact with the wall forms the particle convection, because the heat absorbed (or released) by gas phase is negligible in comparison with the part due to particles. Therefore, the terms of conduction component and particle convection are different from the physical point of view, this is proved by the calculated results in the following subsection.

Regimes of conduction and convection

First, we consider the situation at ambient temperature (300 K), because the radiation is not considered in the Saxena and Ganzha (1984) classification. Figure 2 shows the percentage of conductive component R_d and convective component R_v, as a function of Ar (in logarithmic scale). For the range of

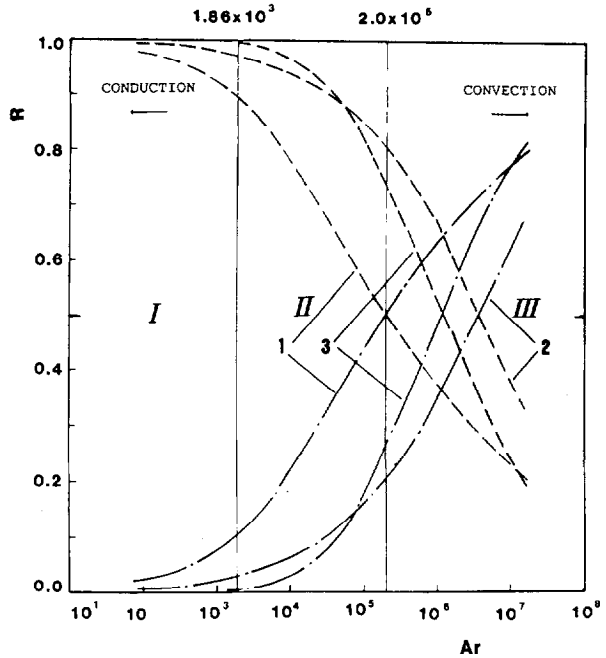

Figure 2 Fraction of conduction and convection *versus* Archimedes number; (– – – R_d; · – · – R_v). 1 = authors' model; 2 = Borodulya et al. (1991) correlation; 3 = Kunii and Levenspiel's (1991) model

Archimedes numbers considered, we use two limits for the definition of heat transfer regimes. One is the criterion to determine whether the conduction mode or convection mode is dominant or not; i.e., $R_d = R_v = 50$ percent. The other is $R_v = 10$ percent, which means the convection is a negligible mode when $R_v \leq 10$ percent. With these two limits, we can divide the heat transfer domain considered in Figure 2 into three regimes.

Regimes I, Ar $\leq 1.86\,10^3$ ($d_p \leq 0.28$ mm for sand). In this regime, the conduction is the main heat transfer mode and the convection can be neglected.

Regime II, $1.86\,10^3 \leq$ Ar $\leq 2.0\,10^5$ ($0.28 \leq d_P \leq 1.35$ mm). Conduction is the dominant heat transfer mechanism but convection is a non-negligible component in this regime.

Regime III, Ar $> 2.0\,10^5$ ($d_P \geq 1.35$ mm). Convection plays the dominant role in this regime.

In the investigated range of Archimedes numbers, where most experimental and theoretical researches have been carried out, (Ar $\geq 1.86\,10^3$) the convection is a non-negligible component ($R_v > 10$ percent).

If we analyze the original paper related to the Saxena and Ganzha (1984) classification, we can discover that the first criterion for a bed of small particles was Ar ≤ 1600 and $Re_{mf} < 1$, which almost corresponds to the criterion of Ar = 1860 proposed in this paper; for this condition, the fluid flow is laminar. The transition for large particle beds was Ar $\geq 1.6 \times 10^6$ where fully developed, turbulent flow exists, and conduction is only a negligible part. Between these two criteria, particles belong to the transitional group. The limit Ar = $16\,10^5$ is strongly different from ours: Ar = $2\,10^5$. In the Saxena and Ganzha classification, the laminar regime was extended to Ar $\leq 2.17\,10^4$ considering the flow through a packed bed is essentially laminar beyond the Reynolds number limit of 1 and up to 10.

It can be found that Saxena and Ganzha (1984) classification was mainly based on the fluid flow and heat transfer in packed beds. Fluidized and packed beds differ from each other in two main characteristics.

(1) The heat absorbed or released by particles near the wall plays a very important role in the heat exchange procedure.
(2) There exists a temperature difference between the gas phase and particles, just as shown in the experimental data of Flamant et al. (1992b) and predicted results of Lu et al. (1993).

The former trend leads to a non-negligible role of conduction even in the range of turbulent regime, and the latter leads to the enhancement of interphase heat transfer due to interstitial fluid flow, even in the nearly laminar regime.

It is interesting to note that Saxena and Ganzha (1984) proposed Ar = $1.3\,10^5$ as a criterion to divide the transition regime into two subgroups. This criterion is roughly in agreement with the crossing point of predicted curves at which convection and conduction represent the same fraction of total heat transfer quantity. Thus, Ar = $2.10\,10^5$ can be used as a criterion to divide the heat transfer domain into two regimes where conduction or convection is dominant.

The fractions of convective and conductive components predicted by the Kunii and Levenspiel's model (1991) and Borodulya et al.'s correlation (1991) are also given in Figure 2. Similar trends by comparison with the authors' model are exhibited, but it seems that lower values of the convection fraction are predicted in general situations. The transition points between the conduction dominant domain and the convection dominant domain are about Ar = $1.26\,10^6$ for the Kunii and Levenspiel's model and Ar = $3.84\,10^6$ with the Borodulya et al.'s (1991) correlation, respectively. The reasons are that the gas convection considered by Kunii and Levenspiel is attributed to the lateral mixing of gas in the void spaces at the wall with adjacent particles and that convection in beds of rather small particles ($d_P = 0.4$ mm) is neglected by Borodulya et al. (1991). However, these three models all predict that conduction is a non-negligible component when Ar $> 1.6 \times 10^6$, even at Ar = $1.75\,10^7$ ($d_P = 6$ mm for sand).

As pointed above, the convection component can be considered as the result of gas flow through the emulsion phase with enhancement of longitudinal convection, transverse dispersion, and interphase heat transfer intensity. Figure 3 indicates the enhancement of the effective conductivity of the gas phase and the interphase heat exchange between gas and particles with the correlations discussed and chosen in Lu et al. (1993). The superscript o means the state $\langle v \rangle = 0$, and the subscript B is related to the state far from the wall because these two parameters change with the distance from the wall. It seems that both parameters increase strongly with the Archimedes number, especially for the relative effective conductivity of the gas phase which, because of the transverse dispersion, increases from 1.37 at Ar = $1.86\,10^3$ to 19.2 at Ar = $2.0\,10^5$.

During the period of emulsion packets contacting with the wall, the heat transferred through the interface between the wall and the emulsion packet is wholly stored (when $T_W > T_B$) inside the emulsion packet if the gas flow is zero. In fact, there exists a gas flow for any conditions in fluidized beds, which carries one part of the heat transferred from the wall out of the considered emulsion packet. Besides the percentages of conduction and convection mode, R_d and R_v, Figure 4 gives the fractions R_o, R_s, R_p, and R_g defined as follows.

(1) R_o is the ratio of heat carried out by the flowing gas to the total heat transferred from the wall.
(2) R_s is the ratio of heat absorbed by the emulsion packet to the total heat transferred from the wall.
(3) R_p is the fraction of heat transferred through the interface between the particle phase and the wall.

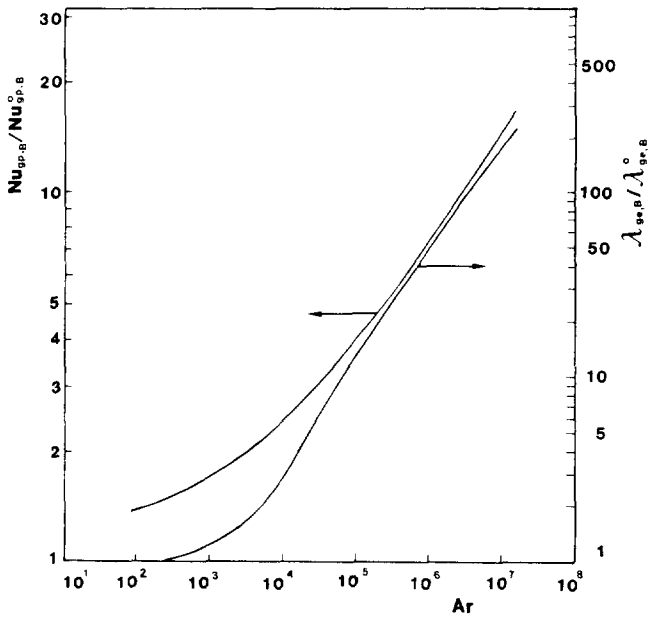

Figure 3 Variations of interphase heat transfer intensity and effective conductivity of gas phase *versus* Archimedes number

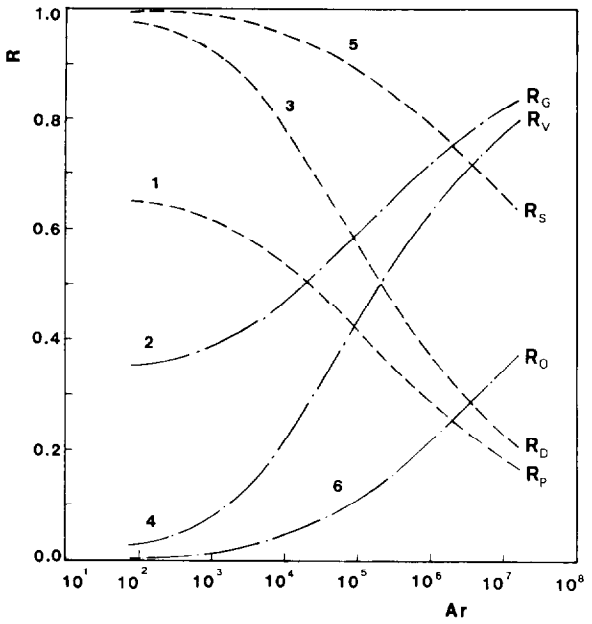

Figure 4 Variations of different heat transfer components *versus* Archimedes number; 1 = R_P; 2 = R_g; 3 = R_d; 4 = R_V; 5 = R_S; 6 = R_O

(4) R_g is the fraction of heat transferred through the interface between the with gas phase and the wall.

$$R_e = E_d + R_v = R_o + R_s = R_p + R_g \qquad (14)$$

We can see two main trends in Figure 4. The ratio R_o increases with the Archimedes number that means the longitudinal convection plays a more and more important role as Ar rises. In addition R_o is much smaller than the percentage of convective component, for example, when Ar = 2.0 10^5, R_o is only 13.5 percent; whereas, R_v = 50 percent and R_g = 62.8 percent. It means that only a minor part of the heat transferred from the wall to the gas phase is carried out by the interstitial gas, the other part is transferred to the particle phase by the interphase heat transfer and is included in the particle convection component. A small part is stored inside the gas, which supports the explanation given above that the conduction component and particle convection are two different terms from the physical point of view.

It should be pointed out that the predicted results shown in Figure 2 are based on the specific bed material and fluidizing fluid as well as on some other parameters shown in Appendix A. We can find from Equations 12 and 13 that several parameters but Ar also affect the heat transfer in fluidized beds. However, the qualitative trends are similar. Therefore, the Archimedes number can be used as a parameter to define the heat transfer domains where the convection and conduction play different roles at ambient temperature.

Heat transfer in high temperature beds

When the temperatures of fluidized beds and heat transfer walls increase, the hydrodynamical and heat exchange characteristics in the beds change because of the dependence of thermophysical properties of fluidizing gas on temperature and to the radiation, which plays an increasingly important role in heat transfer processes. Although heat transfer is closely connected with the hydrodynamics in fluidized beds, we only pay attention here, to the direct influence of temperature on heat transfer, because only a few investigations have been conducted on the dependence of hydrodynamics on temperature up to now. The same formulae given above to determine the bubble fraction are used, although the Reynolds number predicted by Equation 10 is not still the optimum value corresponding to the maximum heat transfer coefficients.

First, we investigate the case of a small temperature difference between the wall and the fluidized bed because the heat transfer obviously depends on the heat flux direction when the temperature difference is large as analyzed in Flamant et al. (1993). Figure 5 shows the predicted results of the fraction of radiative component versus the total heat transfer; i.e., $R_r = \mathrm{Nu}_r/\mathrm{Nu}_W$ in a double-logarithmic coordinate of Archimedes and Planck numbers for the case $T_W/T_B = 0.95$, $\varepsilon_W = 0.8$ and $\varepsilon_P = 0.6$. The three curves R_r = 10 percent and R_r = 50 percent divide the heat transfer domain into three regimes. Radiation can be considered as a negligible component in the regime A above the curve R_r = 10 percent. Whereas radiation is a dominant component in the regime C under the curve R_r = 50 percent. The limit R_r = 50 percent corresponds to the convection/radiation interaction number equal to 1 in Flamant et al. (1992a). For the regime B between these two curves, the conduction/convection modes are dominant, but radiation also plays a significant role in the heat transfer procedure. It is interesting to note that the distance between the two curves is almost the same along the abscissa (Archimedes number), which indicates that the portion of radiation is directly related to the Planck number for the same Archimedes number.

The changes of the ratio between conductive or convective components and the sum of two components, $R_{d/dv} = \mathrm{Nu}_d/(Nu_d + \mathrm{Nu}_V)$ or $R_{V/dv} = \mathrm{Nu}_V/(\mathrm{Nu}_d + \mathrm{Nu}_V)$, are not obvious in comparison with the results at ambient temperature for the same Archimedes number. If we combine the regimes A, B, and C limited by R_r = 10 percent and R_r = 50 percent with the scheme for conduction and convection proposed above, a new scheme of heat transfer regimes can be obtained that considers all heat transfer modes. The different combinations of regimes A, B, C, and I, II, III lead to nine heat transfer domains where each heat transfer mode has a different significance.

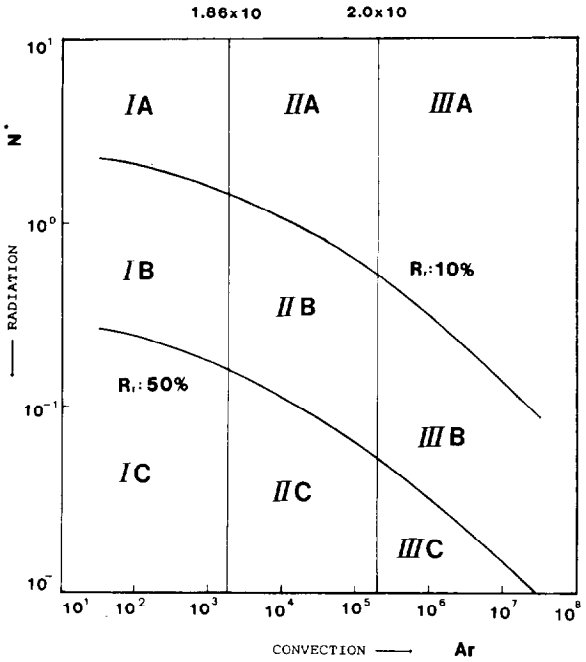

Figure 5 Heat transfer scheme for high temperature beds with $T_W/T_B = 0.95$

Domains

IA: conduction dominant;
IB: conduction dominant and radiation significant;
IC: radiation dominant and conduction significant;
IIA: conduction dominant and convection significant;
IIB: conduction/convection/radiation significant but conduction is more important than convection;
IIC: radiation dominant and conduction + convection significant but convection less important;
IIIA: convection dominant and conduction significant;
IIIB: conduction + convection + radiation significant but convection is more important than conduction; and
IIIC: radiation dominant and conduction/convection significant but conduction less important.

In the above definition of heat transfer domains, the term "dominant" means that the fraction of such component is larger than 50 percent. Comparing the scheme proposed above with the heat transfer diagram presented by Flamant et al. (1992a), who proposed eight domains in a T *versus* d_P diagram, one of the main differences is that there is a domain of radiation dominant (IC) for small Archimedes numbers ($Ar \leq 1.86 \times 10^3$). The reason is that a generalized model is used for the whole Archimedes number range considered in Figure 5 and that two different models were used for the regimes corresponding to $Ar < 1.4\ 10^4$ and $Ar > 1.4\ 10^4$ in the previous work.

The predicted trends shown in Figure 5 are obtained for a small temperature difference between the wall and fluidized beds. In most industrial equipment, the temperature difference is large. In these cases, the heat transfer intensity, as well as the criterion for heat transfer regimes, will be affected by the heat flux direction due to the different dependency of each heat transfer mode on bed or wall temperature. Figure 6 shows the relative fractions of convection and conduction in comparison with the sum of these two components $R_{V/dV}$ and $R_{d/dV}$ for the different temperature ratios $T_W/T_B = 2.0$, 0.95, and 0.5. For the calculation, the thermal properties in the Archimedes number are determined with the bed temperature as the reference

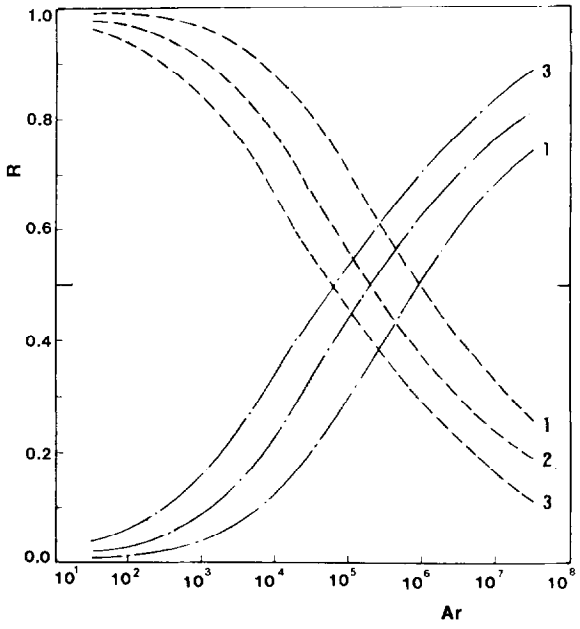

Figure 6 Influence of temperature ratio T_W/T_B on relative significance of conduction and convection; ---- $R_{d/dV}$; -·-·- $R_{V/dV}$; 1 = T_W/T_B = 2.0; 2 = T_W/T_B = 0.95; 3 = T_W/T_B = 0.5

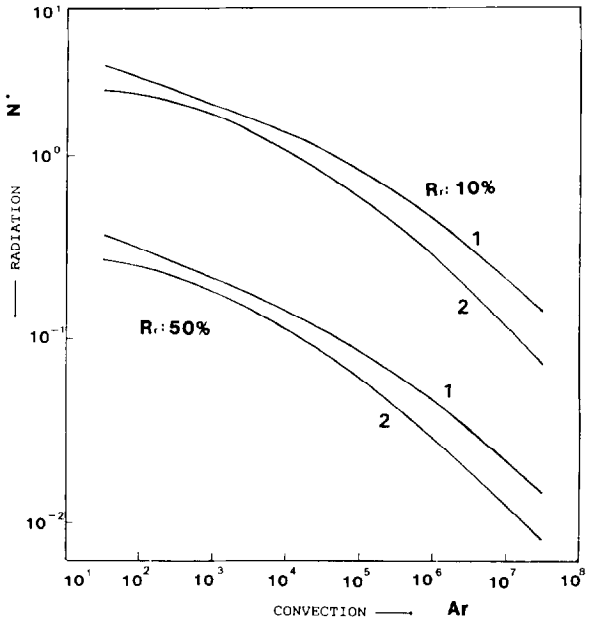

Figure 7 Influence of temperature ratio T_W/T_B on relative importance of radiation; 1 = T_W/T_B = 2.0; T_W/T_b = 0.5

temperature, because the hydrodynamics in the bed is determined by the bed temperature. It can be found that the fraction of convective component is much smaller for $T_W/T_B = 2.0$ than for $T_W/T_B = 0.5$ for the same Archimedes number. The reasons of this trend are that convection is enhanced with a decrease of wall temperature and that conduction is strengthened by an increase of wall temperature. A detailed discussion on the dependency of each component on temperature was given in Flamant et al. (1993).

Considering the influence of the heat flux direction on the heat transfer regimes including radiation, it can be seen in Figure 7 that for given values of the Archimedes number and of the radiation fraction, the Planck number, which indicates the ratio of conduction with respect to radiation, is larger for $T_W/T_B = 2.0$ than for $T_W/T_B = 0.5$. This means that conduction plays a more important role in heat transfer process when T_W is larger than T_B than when T_W is lower than T_B, which is in agreement with the trend shown in Figure 6.

It should be pointed out that predicted results given above are obtained for the values of the parameters $\varepsilon_W = 0.8$ and $\varepsilon_P = 0.6$ that is a typical case in experimental researches and industrial equipment. However, the radiation is influenced strongly by these two parameters, especially by the wall emissivity ε_W (Flamant et al. 1993).

Conclusion

On the basis of the authors' recent model, a heat transfer classification scheme in bubbling gas–solid fluidized beds is discussed from the point of view of heat transfer mechanisms. First a discussion is given for the distinction between the definitions of conduction and particle convection. It is shown that the dimensionless Archimedes and Planck numbers are the practical parameters for analyzing the variation of the heat transfer modes (conduction, convection, and radiation) as functions of particle diameter and temperature. The solutions of heat transfer equations give the value of all components as functions of Archimedes number. At ambient conditions, the results prove that conduction is dominant and convection is

negligible for Ar < $1.86\ 10^3$ and that convection is dominant for Ar > $2\ 10^5$. These limits correspond for sand to $d_P = 280\ \mu$m and $d_P = 1.35$ mm, respectively, which is in good agreement with the conclusion of Decker and Glicksman (1981). We can consider that this paper demonstrated quantitatively the Saxena and Ganzha (1984) classification scheme for ambient condition. However, a significant difference is shown. We propose the limit Ar = $2.0\ 10^5$ for dominant convection; whereas, in Saxena and Ganzha (1984), the value Ar = $1.3\ 10^5$ is the transition for large but not dominant convective contribution. This difference is mainly because of gas–solid heat transfer contribution included in our model. At the same time, it is predicted in the present model that both conduction and convection are non-negligible components of heat transfer in the range $1.86\ 10^3 \leq \mathrm{Ar} \leq 10^8$. By comparison with other works, for example Kunii and Levenspiel (1992), Borodulya et al. (1991), we are agree to predict the existence for significant conductive heat transfer in the whole range of Archimedes number (even for very large values). The influence of radiation is illustrated in a conduction/radiation interaction number (N^*, modified Planck number) *versus* Archimedes number plot. For example, radiation becomes significant at $N^* = 0.5$ and dominant at $N^* = 0.055$ for Ar = $2.0\ 10^5$, which corresponds to $d_P = 2.15$ mm, $T_B = 548$ K and $d_P = 3.84$ mm, $T_B = 1148$ K, respectively. The combination of the conclusions related to conduction, convection, and radiation contribution leads to a heat transfer regime diagram divided in nine domains in an N^* *versus* Ar representation. In this diagram, the locations of the limits between the domains vary with the heat flux direction and the temperature difference between the bed and the wall. The convective component percentage increases with the bed-to-wall temperature difference and decreases when the wall is at higher temperature than the bed. For the same value of Archimedes number, the radiation component percentage is smaller in the case $T_W > T_B$ than in the case $T_W < T_B$.

References

Baskakov, A. P., Berg, B. V., Vitt, O. K., Filippovsky, N. F., Kirakosyan, V. A., Goldobin, J. M. and Maskaev, V. K. 1973. *Powder Technol.*, **8**, 273–282

Borodulya, V. A., Ganzha, V. L., Teplitsky, Yu. S. and Epanov, Yu. G. 1985. *J. Eng. Phys.*, **49**, 621–626

Borodulya, V. A., Teplitsky, Yu. S., Markevich, I. I., Hassan, A. and Yeryomenko, T. P. 1991. *Ind. Eng. Chem. Res.*, **30**, 47–53

Chen, P. and Pei, D. C. T. 1985. *Int. J. Heat Mass Transfer*, **28**, 675–682

Decker, N. A. and Glicksman, C. R. 1981. *AIChE Symp. Ser.*, **77**, 341–349

Flamant, G., Fatah, N. and Flitris, Y. 1992a. *Powder Technol.*, **69**, 223–230

Flamant, G., Fatah, N., Olalde, G. and Hernandez, D. 1992b. *J. Heat Transfer*, **14**, 50–55

Flamant, G., Lu, J. D. and Variot, B. 1993. *Chem. Eng. Sci.*, **48**, 2493–2503

Flamant, G., Lu, J. D. and Variot, B. 1994. *J. Heat Transfer*, **116**, 652–660

Geldart, D. 1973. *Powder Technol.*, **7**, 285–292

Jovanovic, G. and Catipovic, N. 1983. *Fluidization IV, Eng. Found. Ann. Rept.*, 69–76

Kunii, D. and Levenspiel, O. 1992. *Ind. Eng. Chem. Res.*, **30**, 136–141

Lu, J. D. 1988. Ph.D. thesis, Huazhong University of Science and Technology, Wuhan, China

Lu, J. D., Flamant, G. and Snabre, P. 1993. *Chem. Eng. sci.*, **48**, 2479–2492

Ozkaynak, T. F. and Chen, J. C. 1980. *AIChE J.*, **26**, 544–550

Saxena, S. C. and Ganzha, V. L. 1984. *Powder Technol.*, **39**, 199–208

Thring, R. H. 1977. *Int. J. Heat Mass Transfer*, **20**, 911–918

Appendix A

Physical properties of air

$\rho_g = (351/T)k_g/\mathrm{m}^3$
$\lambda_g = 5.66\ 10^5 T + 1.1\ 10^{-2} W/(\mathrm{mK})$
$C_{pg} = (0.99 + 1.22\ 10^{-5} T - 5.68\ 10^{-2}) \times 10^3 \mathrm{J/(kg \cdot K)}$
$\mu_g = 0.42 \times 10^{-6} T^{2/3} \mathrm{N \cdot s/m^2}$

Physical properties of sand

$\rho_s = 2500\ \mathrm{kg/m^3}$
$\lambda_s = 1.75\ \mathrm{W/(m \cdot K)}$
$C_{ps} = 860\ \mathrm{J/(kg \cdot K)}$
$\varepsilon_p = 0.6$

Other calculating parameters

$\delta_{mf} = 0.4$
$\varepsilon_w = 0.8$
$\phi_P = 1.0$
$L = 20$

Appendix B (from Flamant et al. 1993)

Boundray conditions for Equations 1–4

$\mathrm{Fo} = 0^-,\ \theta_g = \theta_P = T_B/T_m$
$Y = 0,\ \theta_g = \theta_B = T_B/T_m$
$X = 0,\ \theta_g = \theta_P = T_w/T_m$
$V = 0$

$$I_i = \varepsilon_w \frac{\theta_w^4}{\pi} + 2(1 - \varepsilon_w) \sum_{j=i}^{N/2} I_j W_j |\mu_j| \qquad (i - N/2,\ N)$$

$X \to \infty \theta_g = \theta_P = T_B/T_m$
$V = 1$

$$\frac{\partial I_i}{\partial X} = 0 \quad (i = N/2 + 1,\ N)$$

$I_l = I_{N/2+l} \qquad (i = 1,\ N/2)$

Correlations for the estimation of parameters used in Equations (1–3); porosity distribution near heat transfer walls

$\delta = 1 - 3(1 - \delta_{eB})(X - 2X^2/3) \qquad X \leq 1$
$\delta = \delta_{eB} \qquad X > 1$

Effective conductivity of gas phase and particle phase

$\lambda_{ge}/\lambda_g = 1 - (1 - \delta_{eB})^{1/2} - \delta_{eB} + 0.1\ \mathrm{Re\ Pr} XV \qquad X < 1$
$\lambda_{ge}/\lambda_g = 1 - (1 - \delta_{eB})^{1/2} + 0.1\ \mathrm{Pe\ Pr}\ V \qquad X > 1$

$$\frac{\lambda_{Pe}}{\lambda_g} = [(1 - \delta_{eB})^{1/2} + \delta_{eB} - \delta] \frac{2}{(1 - B/\gamma)} \left[\frac{(1 - 1/\gamma)B}{(1 - B/\gamma)^2} \ln\left(\frac{\gamma}{B}\right) - \frac{B + 1}{2} - \frac{B - 1}{(1 - B/\gamma)} \right]$$

with $\gamma = \lambda_e/\lambda_g$ and $B = 1{,}25\ [(1 - \delta)/\delta]^{10/9}$ for packed bed of spheres.

Heat transfer between two phases

$$\mathrm{Nu}_{gP} = (7 - 10\delta + 5\delta^2)(1 + 0.7\mathrm{Re}^{0.2}\mathrm{Pr}^{1/3}) + (1.33 - 2.4\delta + 1.2\delta^2)\mathrm{Re}^{0.7}\mathrm{Pr}^{1/2}.$$